Characterization and Reactivity of the Tetrametallic Pd$_2$-Mo$_2$ Complex Ph(Bu)P(η^5-C$_5$H$_4$)Mo(CO)$_3$Pd(μ-I)$_2$PdMo(CO)$_3$(η^5-C$_5$H$_4$)P(Ph)Bu and Its Use to Model Pd-Catalyzed Cross-Coupling Reactions Leading to M−C≡C Bonds

Francesco Angelucci,[†] Antonella Ricci,[†] Dante Masi,[‡] Claudio Bianchini,[‡] and Claudio Lo Sterzo*,[§]

Istituto CNR di Metodologie Chimiche (IMC-CNR), Sezione Meccanismi di Reazione Dipartimento di Chimica, Box 34-Roma 62, Università "La Sapienza", Piazzale Aldo Moro 5, 00185 Roma, Italy, Istituto CNR di Chimica dei Composti Organo Metallici (ICCOM), Area della Ricerca CNR, Via Madonna del Piano snc, 50019 Sesto Fiorentino, Firenze, Italy, and Dipartimento di Scienze degli Alimenti, Facoltà di Agraria, Università degli Studi di Teramo, Via Spagna 1, 64023-Mosciano Sant'Angelo, Teramo, Italy

The mechanism of the Pd-catalyzed cross-coupling reaction between tributyltin acetylides and metal iodides has been investigated with the use of a model Mo precursor bearing a ligand with appropriate steric and electronic properties. This study has allowed us to intercept the tetrametallic Pd$_2$-Mo$_2$ complex Ph(Bu)P(η^5-C$_5$H$_4$)Mo(CO)$_3$Pd(μ-I)$_2$PdMo(CO)$_3$(η^5-C$_5$H$_4$)-P(Ph)Bu, which is a precursor to the catalytically active solvento complex Ph(Bu)P(η^5-C$_5$H$_4$)Mo(CO)$_3$PdI(DMF). Both complexes play a key role in Pd-catalyzed cross-coupling reactions between tributyltin acetylides and metal iodides, leading to metal-σ-alkynyls. The catalytic cycle for such a reaction has been further elucidated, especially with regard to the role of the ligands in the metal iodide for the stabilization and/or detection of the intermediates as well as for the formation of the M-alkynyl product.

Introduction

Palladium-catalyzed bond-forming reactions play a relevant role in synthetic organic and organometallic chemistry as well as in homogeneous catalysis.[1] Our contribution to this field has recently culminated in the discovery of a metal−carbon coupling reaction that allows for the catalytic formation of M−C≡C moieties from tributyltin acetylides and metal iodides.[2] From qjthe practical viewpoint, this reaction provides a surprisingly efficient method for the synthesis of highly ethynylated organometallic compounds of great interest in material science.[3] From the fundamental perspective, understanding the mechanism of this reaction[4] would provide a unique opportunity to get insight into a var-

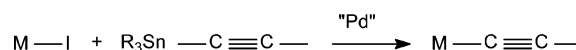$$M—I \ + \ R_3Sn—C≡C— \ \xrightarrow{\text{"Pd"}} \ M—C≡C—$$

Figure 1. Pd-promoted metal−carbon bond-formation process.

iety of palladium-promoted bond-formation processes, some of which are still the object of intense debate.[5,6]

The reaction mechanism of the Pd-promoted coupling of metal iodides with tributyltin acetylides (Figure 1) has been extensively studied with the use of model metal iodides such as **1a**,**b** (Figure 2).

Important species involved in the catalytic cycle, such as the oxidative-addition products (**2a**,**b**) and the transmetalation intermediates (**7a**,**b**), have been intercepted, while the presence of phosphorus ligands in the model compounds has allowed the use of ^{31}P NMR spectroscopy to unravel several steps in the catalytic process.[4d] Over-

---

* Corresponding author. E-mail: losterzo@unite.it.
[†] Istituto CNR di Metodologie Chimiche.
[‡] Istituto CNR di Chimica dei Composti Organo Metallici.
[§] Dipartimento di Scienze degli Alimenti, Facoltà di Agraria, Università degli Studi di Teramo.

(1) Schlosser, M. *Organometallics in Synthesis*; John Wiley & Sons Ltd.: Chichester, England, 1994. (b) Heck, R. F. *Palladium in Organic Synthesis*; Academic Press: New York, 1985. (c) Tsuji, J. *Palladium Reagents and Catalysts. Innovation in Organic Synthesis*; John Wiley & Sons Ltd.: Chichester, England, 1996. (d) Mitchell, T. N. In *Metal-catalyzed Cross-coupling Reactions*; Diederich, F., Stang, P. J. Eds.; Wiley-VCH: Weinheim, Germany, 1998. (e) *J. Organomet. Chem.* **2002**, *653* (issue 1−2), Special Issue, 30 Years of the Cross-Coupling Reaction.
(2) Lo Sterzo, C. *J. Chem. Soc., Dalton Trans.* **1992**, 1989. (b) Lo Sterzo, C. *Synlett* **1999**, 1704. (c) Crescenzi, R.; Lo Sterzo, C. *Organometallics* **1992**, *11*, 4301. (d) Viola, E.; Lo Sterzo C.; Crescenzi, R.; Frachey, G. *J. Organomet. Chem.* **1995**, *493*, 55. (e) Viola, E.; Lo Sterzo C.; Crescenzi, R.; Frachey, G. *J. Organomet. Chem.* **1995**, *493*, C9.

(3) Viola, E.; Lo Sterzo, C.; Trezzi, F. *Organometallics* **1996**, *15*, 4352. (b) Buttinelli, A.; Viola, E.; Antonelli, E.; Lo Sterzo, C. *Organometallics* **1998**, *17*, 2574. (c) Antonelli, E.; Rosi, P.; Lo Sterzo, C.; Viola, E. *J. Organomet. Chem.* **1999**, *578*, 210. (d) Altamura, P.; Giardina, G.; Lo Sterzo, C.; Russo, M. V. *Organometallics* **2001**, *20*, 4360. (e) La Groia, A.; Ricci, A.; Bassetti, M.; Masi, D.; Bianchini, C.; Lo Sterzo, C. *J. Organomet. Chem.* **2003**, *683*, 406.
(4) Spadoni, L.; Lo Sterzo, C.; Crescenzi, R.; Frachey, G. *Organometallics* **1995**, *14*, 3149. (b) Cianfriglia, P.; Narducci, V.; Lo Sterzo, C.; Viola, E.; Bocelli, G.; Kodenkandath, T. A. *Organometallics* **1996**, *15*, 5220. (c) Tollis, S.; Narducci, V.; Cianfriglia, P.; Lo Sterzo, C.; Viola, E. *Organometallics* **1998**, *17*, 2388. (d) Ricci, A.; Angelucci, F.; Bassetti, M.; Lo Sterzo, C. *J. Am. Chem. Soc.* **2002**, *124*, 1060. (e) Ricci, A.; Lo Sterzo, C. *J. Organomet. Chem.* **2002**, *653*, 177. (f) Angelucci, F.; Ricci, A.; Lo Sterzo, C.; Masi, D.; Bianchini, C.; Bocelli, G. *Organometallics* **2002**, *21*, 3001.
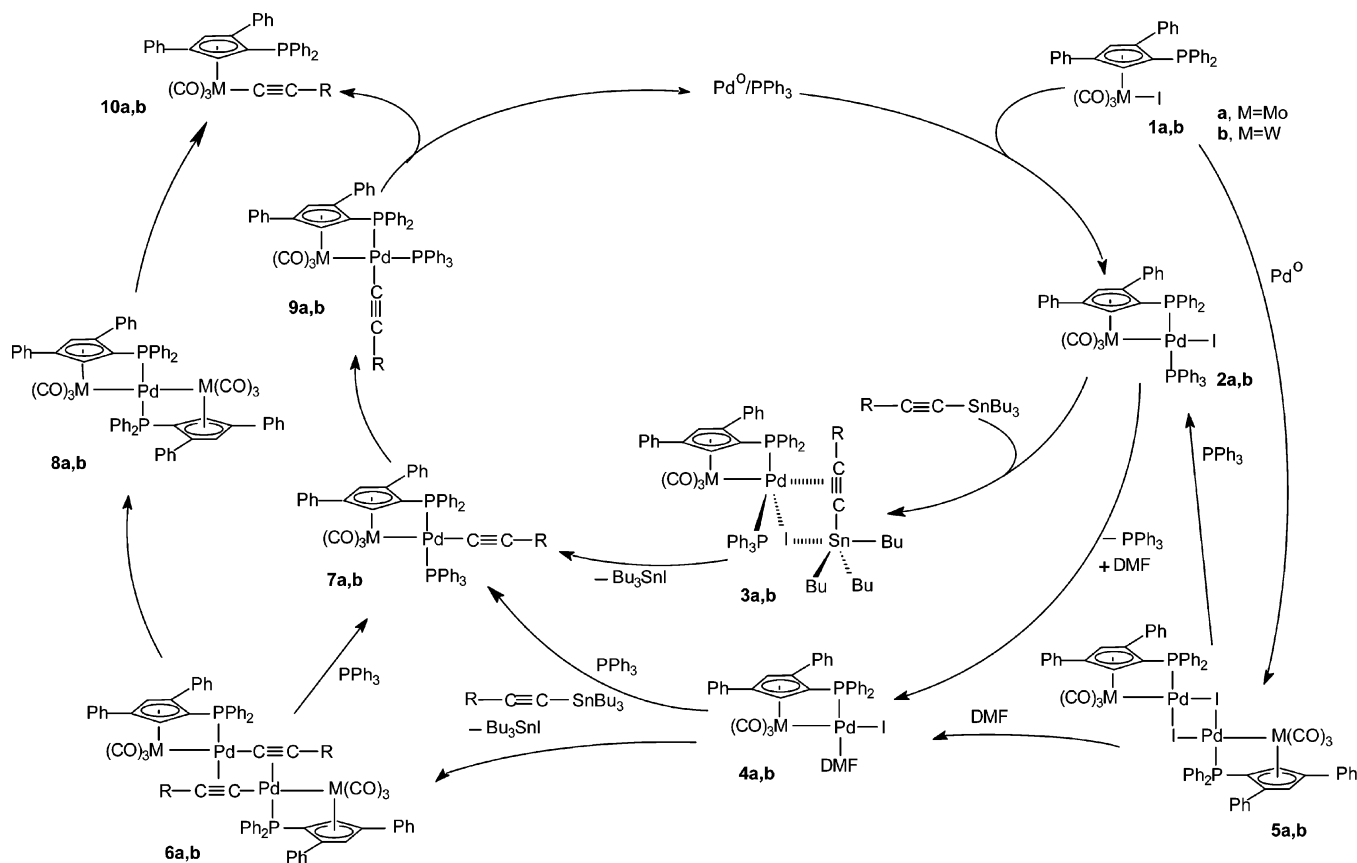
Figure 2. Full picture of the catalytic cycle of the Pd-promoted metal–carbon (M–C≡C) bond-formation process.

all, the spectroscopic and kinetic investigation has provided the following information: (i) at high initial concentrations of the oxidative-addition intermediate **2a,b** ($\cong 10^{-2}$ M), the transmetalation proceeds through the formation of a π-alkynyl adduct (**3a,b**) between **2a,b** and the organostannane $Bu_3Sn-C\equiv C-R$; (ii) at low initial concentrations of **2** ($\cong 10^{-4}$ M), the reaction proceeds through the formation of the highly reactive solvento complex **4**; (iii) in the absence of PPh_3, the DMF adducts **4a,b**, **5a,b**, and **6a,b** are formed, leading to a coupling process that involves the trimetallic species **8a,b**.[4f,7] Important electronic effects have also been observed by replacing PPh_3 with other tertiary phosphines.[4d]

Aimed at elucidating further the catalytic mechanism, we decided to carry out a systematic study of the cross-coupling reaction by varying the electronic and steric properties of the metal iodide precursors. To this purpose, we have designed and developed a synthetic strategy to a Mo iodide bearing a cyclopentadienyl ligand devoid of phenyl substituents and containing a tertiary phosphine arm where a *n*-butyl group replaces a phenyl group.

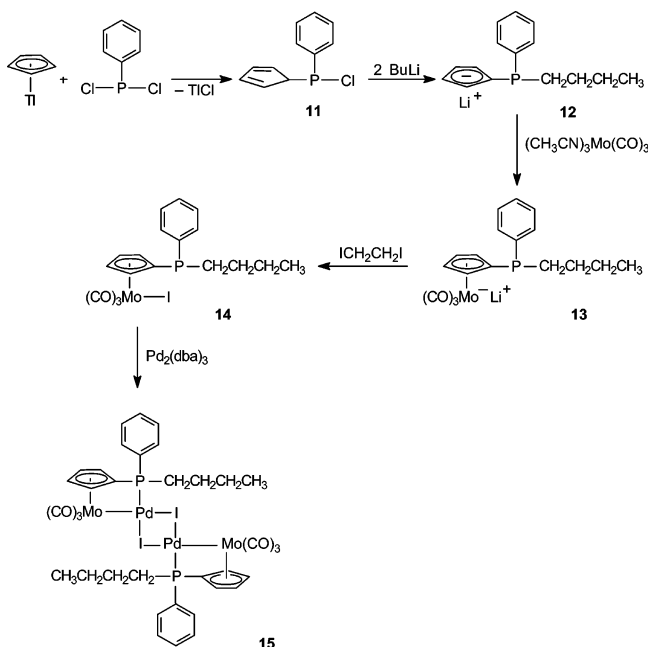The results of this study are reported in this paper.

Results and Discussion

The synthetic protocol developed to prepare the phenyl(butyl)cyclopentadienylphosphino ligand **12** and the corresponding Mo and the Mo–Pd complexes **14** and **15** is illustrated in Scheme 1.

A procedure previously reported by Cullen[9a] was adapted to prepare chloro(phenyl)cyclopentadienylphosphine (**11**), by the reaction of CpTl with dichlorophosphine[9b,c] in a molar ratio of 1:1, followed by treatment with BuLi (2 equiv) to give **12** as the major product. The use of 2 molar equiv of BuLi with respect to **11** allowed for both the substitution of butyl for chloride and the deprotonation of the cyclopentadienyl ring. Subsequent reaction of **12** with $(CH_3CN)_3Mo(CO)_3$ gave **13**, which was converted to **14** by reaction with 1,2-diiodoethane. The formation of **14** was unambiguously shown by in

(5) Farina, V.; Krishnamurthy, V.; Scott, W. J. *The Stille Reaction*; John Wiley & Sons: New York, 1998. (b) Gillie, A.; Stille, J. K. *J. Am. Chem. Soc.* **1980**, *102*, 4933. (c) Tatsumi, K.; Hoffmann, R.; Yamamoto, A.; Stille, J. K. *Bull. Chem. Soc. Jpn.* **1981**, *54*, 1857. (d) Stang, P. J.; Kowalski, M. H.; Schiavelli, M. D.; Longford, D. *J. Am. Chem. Soc.* **1989**, *111*, 3347. (e) Brown, J. M.; Cooley, N. A. *Organometallics* **1990**, *9*, 353. (f) Farina, V.; Krishnan, B.; Marshall, D. R.; Roth, G. P. *J. Org. Chem.* **1993**, *58*, 5434. (g) Amatore, C.; Jutand, A.; Suarez, A. *J. Am. Chem. Soc.* **1993**, *115*, 9531, and references therein. (h) Morita, D. K.; Stille, J. K.; Norton, J. R. *J. Am. Chem. Soc.* **1995**, *117*, 8576, and references therein. (i) Amatore, C.; Carré, E.; Jutand, A.; Tanaka, H.; Ren, Q.; Torii, S. *Chem. Eur. J.* **1996**, *2*, 957. (j) Mateo, C.; Cárdenas, D. J.; Fernández-Rivas, C.; Echavarren, A. M. *Chem. Eur. J.* **1996**, *2*, 1596. (k) Amatore, C.; Broeker, G.; Jutand, A.; Khalil, F. *J. Am. Chem. Soc.* **1997**, *119*, 5176. (l) Louie, J.; Hartwig, J. F. *J. Am. Chem. Soc.* **1995**, *117*, 11598. (m) Hartwig, J. F. *Angew. Chem., Int. Ed.* **1998**, *37*, 2046.

(6) Farina, V.; Krishnan, B. *J. Am. Chem. Soc.* **1991**, *113*, 9585. (b) Casado, A. L.; Espinet, P. *J. Am. Chem. Soc.* **1998**, *120*, 8978. (c) Casado, A.; Espinet, P.; Gallego, A. M. *J. Am. Chem. Soc.* **2000**, *122*, 11771. (d) Casado, A. L.; Espinet, P.; Gallego, A. M.; Martinez-Ilarduya, J. M. *Chem. Commun.* **2001**, 339. (e) Amatore, C.; Bucaille, A.; Fuxa, A.; Jutand, A.; Meyer, G.; Ndedi Ntepe, A. *Chem. Eur. J.* **2001**, 2134. (f) Casares, J. A.; Espinet, P.; Salas, G. *Chem. Eur. J.* **2002**, 4844.

(7) In another context, the field of trimetallic arrays of type M–M′–M was early pioneered by Braunstein.[8]

(8) Barbier, J. P.; Braunstein, P. *J. Chem. Res (S)* **1978**, 412. (b) Bender, R.; Braunstein, P.; Jud, J. M.; Dusausoy, Y. *Inorg. Chem.* **1983**, *22*, 3394, and references therein.

(9) Butler, I. R.; Cullen, W. R.; Rettig, S. J. *Organometallics* **1987**, *6*, 872. (b) Mathey, F.; Lampin, J. P. *Tetrahedron* **1975**, *31*, 2685. (c) Deschamps, B.; Mathey, F. *Phosphorus Sulfur* **1983**, *17*, 317.
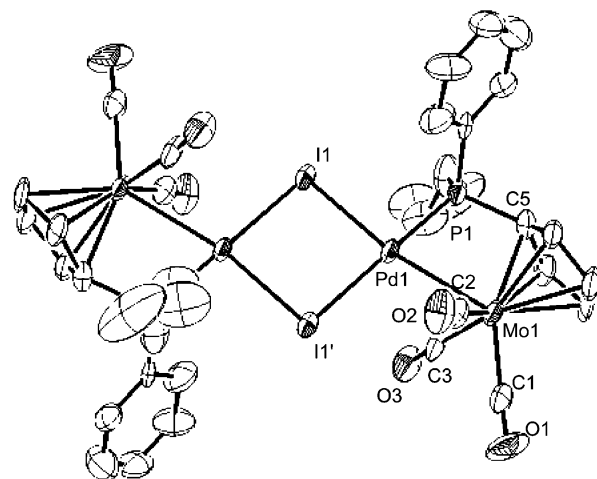
Scheme 1

Figure 3. ORTEP drawing of **15b**.

Table 1. Crystal Data and Structure Refinement for 15b

empirical formula	$C_{18}H_{18}IMoO_3PPd$
fw	642.53
temperature	20 °C
wavelength	1.54180 Å
cryst syst	monoclinic
space group	$P2_1/c(14)$
unit cell dimens	$a = 12.216(3)$ Å
	$b = 9.4250(10)$ Å
	$c = 18.315(7)$ Å
	$\alpha = 90°$
	$\beta = 104.06(3)°$
	$\gamma = 90°$
volume	2045.5(10) Å³
Z	4
density (calcd)	2.086 Mg/m³
absorp coeff	24.819 mm⁻¹
$F(000)$	1224
cryst size	$0.47 \times 0.12 \times 0.10$ mm³
θ range for data collection	3.73 to 54.99°
index ranges	$-12 \leq h \leq 12, 0 \leq k \leq 10,$
	$0 \leq l \leq 19$
no. of reflns collected	2633
no. of indep reflns	2536 [R(int) = 0.0583]
completeness to $\theta = 54.99°$	99.0%
max. and min. transmn	0.1904 and 0.0302
refinement method	full-matrix least-squares on F^2
no. of data/restraints/params	2536/0/217
goodness-of-fit on F^2	1.147
final R indices [$I > 2\sigma(I)$]	R1 = 0.0794, wR2 = 0.1840
R indices (all data)	R1 = 0.0993, wR2 = 0.1988
largest diff peak and hole	1.310 and −1.474 e Å⁻³

situ ³¹P NMR spectroscopy,[10] yet all our attempts to isolate this compound in analytically pure form were unsuccessful.[11] Therefore, Pd₂(dba)₃ was directly added to the crude reaction mixture containing **14** to give the μ-I tetrametallic complex **15** in 22% yield.

Compound **15** shows some remarkable NMR characteristics. The ³¹P{¹H} NMR spectrum in CDCl₃ consists of two distinct singlets at 46.7 and 47.2 ppm, which are due to the diastereomers *rac dl* (**15a**) and *meso* (**15b**) generated by the two stereogenic phosphorus centers.

The presence of two diastereomers is also evident in the ¹H NMR spectrum. In the 5.6–4.0 ppm region, six well-separated signals are present; four signals (1H intensity) out of the six are attributable to the α and α′ Cp protons of each diastereomer, while the remaining two signals (2H intensity) are assigned to the β and β′ Cp protons of either diastereomer. With regard to the butyl substituent attached to the stereogenic phosphorus centers, it is worth noticing that distinct signals are observed for the methylene groups of each diastereomer as well as for the terminal methyl groups.

Recrystallization of the diastereomeric mixture **15** by the liquid-diffusion method (CH₂Cl₂−pentane) gave a red crystalline solid of the *meso* form **15b**, well suited for a single-crystal X-ray diffraction analysis.

X-ray and NMR Structural Characterization of 15b and its PPh₃ Derivative 18. The molecular structure of **15b** is shown in Figure 3, while crystal and structural refinement data are listed in Table 1. In the complex, two equivalent bimetallic (Mo−Pd) units are symmetrically bridged by two iodide ligands. In addition

to direct Mo−Pd bonds, each bimetallic Mo−Pd unit is held together by an η⁵-cyclopentadienyl-η¹-phenylbutylphosphino ligand, which binds Mo with the η⁵-Cp ligand and Pd with the phosphorus atom. Three CO groups complete the coordination sphere of molybdenum, while the two bridging iodide atoms complete the square-planar coordination geometry around palladium.

Only a few examples of crystal structures containing a metal−metal bond incorporated into a four-membered ring (under the convention that Cp acts as a single unit ligand) have been reported in the literature.[4b,12]

The Mo−Pd distance is 2.79 Å (Table 2) and is consistent with a single metal−metal bond;[13] the Pd−Pd distance is 3.89 Å, which excludes any bonding interaction between the two metal centers.[14] The struc-

(10) Typically a ³¹P NMR check was performed by loading a sample of the reaction mixture (0.4 mL) in a 5 mm NMR tube, then CDCl₃ (0.01 mL) was added to the solution to provide the lock signal. A prevalent signal at −27.2 ppm attributable to **14** is present in the spectrum.

(11) Complex **14** was very sensitive and its isolation was hampered by the invariable formation of the corresponding phoshinoxide derivative. Evidently the absence of the stabilizing phenyl groups on Cp and the presence of the electron-donor butyl group on phosphorus have dramatically increased the sensitivity of complex **14** with respect to the similar, more stable compounds **1** and **2**.

(12) Arena, G. C.; Rotondo, E.; Faraone, F.; Lanfranchi, M.; Tiripicchio, A. *Organometallics* **1991**, *10*, 3874.

(13) Wheatley, N.; Kalck, P. *Chem. Rev.* **1999**, *99*, 3379.

Table 2. Selected Bond Distances (Å) and Angles (deg) for 15b

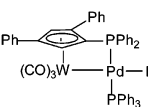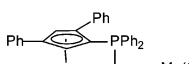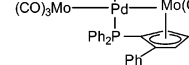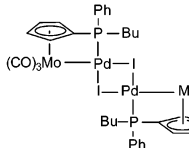|	
Pd(1)−P(1)	2.207(6)
Pd(1)−I(1)	2.6749(18)
Pd(1)−I(1)′	2.721(2)
Pd(1)−Mo(1)	2.787(2)
P(1)−C(5)	1.78(2)
P(1)−Pd(1)−I(1)	93.51(15)
P(1)−Pd(1)−I(1)′	177.53(17)
I(1)−Pd(1)−I(1)′	87.82(6)
P(1)−Pd(1)−Mo(1)	75.08(15)
Pd(1)−I(1)−Pd(1)′	92.18(6)
C(5)−P(1)−Pd(1)	109.9(8)
O(1)−C(1)−Mo(1)	177(3)
O(2)−C(2)−Mo(1)	173(2)
O(3)−C(3)−Mo(1)	175(2)
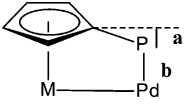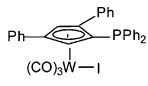
ture exhibits a crystallographic center of symmetry at the midpoint between the bridging iodides. The geometry of the Pd_2I_2 core is characterized by a slightly acute I−Pd−I angle (87.8°) and a slightly obtuse Pd−I−Pd angle (92.2°), values that are in line with those reported for other structures bearing a similar Pd_2I_2 core.[15] The Pd−P distance (2.21 Å) is in the expected range.[15c]

The central Pd_2I_2 unit exhibits an almost regular square-planar geometry. In contrast, severe distortions affect the P−Pd−Mo−Cp cycle, likely due to the strong Pd−Mo and Pd−P bonds (Table 2) and to the steric pressure of the CO ligands. Indeed, the P1−Pd1−I1′ (177.5°) and P1−Pd1−I1 (93.5°) angles deviate appreciably from the ideal values, while the Pd1−I1′ and Pd1−I1 distances, (2.72 and 2.67 Å, respectively) are longer than those reported for similar systems devoid of surrounding bulky ligands.[14a,15c] Moreover, the $Cp_{centroid}$−Mo1−Pd1 angle measures only 110.7°, while the $Cp_{centroid}$−Mo1−C1, the $Cp_{centroid}$−Mo1−C2, and the $Cp_{centroid}$−Mo1−C3 angles are significantly larger (122.9°, 125.1°, and 125.8°, respectively). The steric influence of the CO groups on the bridging iodines is made evident by the deviation from linearity of the Mo−C−O bonds. The Mo1−C3−O3 and the Mo1−C2−O2 angles measure 175° and 173°, respectively, while the Mo1−C1−O1 angle, away from the iodine, is 177°. Therefore, like palladium, a significant distortion affects the octahedral coordination geometry of each molybdenum.

A comparison of the structural data of **15b** with those of the related compounds **1b**, **2b**, **8a**, and **8b** reveals some interesting features. Table 3 reports the deviation of the phosphorus atom from the Cp plane (***a*** values) and the P−Pd bond distance (***b*** values) for all these compounds. Compound **15b** exhibits the largest ***a*** value and the smallest ***b*** value, which is attributed to the strong P−Pd interaction caused by the increased nucleophilicity of the butyl-substituted P atom.

Interestingly, the same $^{31}P\{^1H\}$ NMR spectrum of **15** characterized by two singlets was obtained by dissolving a pure sample of the *meso* stereoisomer **15b** in $CDCl_3$. We interpret this phenomenon as due to a fast and reversible opening of the iodine bridges that would reclose the bridge forming both stereoisomers. However, no NMR signal attributable to a bimetallic "open" form

Table 3. Out-of-Plane Lowering of P Atoms and P−Pd Bond Distances for a Family of Structurally Related Compounds

		a (Å)	***b*** (Å)
	1b	0.15	
	2b	0.58	2.28
	8a (M=Mo)	0.63 0.54	2.33 2.33
	8b (M=W)	0.54 0.59	2.33 2.32
	15b	0.72	2.21

Scheme 2
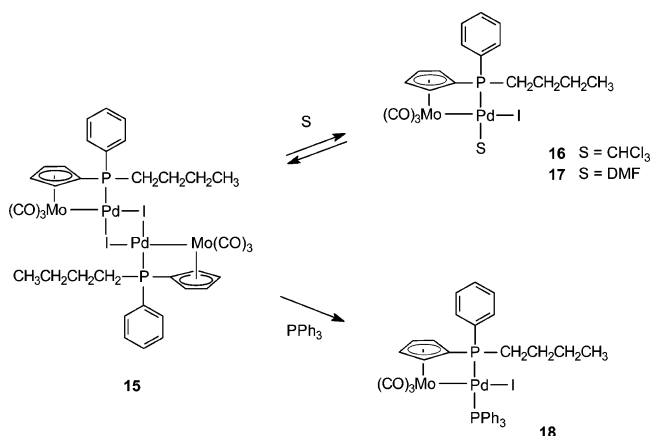
such as that of **16** (S = $CHCl_3$) was observed (Scheme 2). On the other hand, when **15** was dissolved in DMF, a signal at 49.8 ppm appeared in the spectrum, which was safely assigned to the solvento bimetallic complex **17** (S = DMF).[16] This signal was flanked by two less intense signals due to **15a** and **15b**. Apparently, the stabilization of **17** is a consequence of the much better coordinating ability of DMF as compared to chloroform. Within this context, it is worth mentioning that the binuclear complex $[Ph_2Pd_2(\mu^2\text{-}I)_2(AsPh_3)_2]$ has been reported to undergo splitting in DMF to form the solvento complex $PhPdI(AsPh_3)(DMF)$, which is a highly

(14) Thiele, G.; Brodersen, K.; Krause, E. Holle B. *Chem. Ber.* **1968**, *101*, 2771. (b) Brunet, L.; Mercier, F.; Ricard, L.; Mathey, F. *Angew. Chem., Int. Ed. Engl.* **1994**, *33*, No. 7.
(15) Mason, R.; Wheller, A. G. *J. Chem. Soc. A* **1968**, 2549. (b) Holden, J. R.; Baezinger, N. C. *J. Am. Chem. Soc.* **1955**, *77*, 4987. (c) Clark, G. R.; Orbell, J. D. *J. Organomet. Chem.* **1981**, *215*, 121.

(16) Attribution of the ^{31}P NMR peak at 49.8 ppm to the DMF-coordinated species **17** was based on the close similarity to the chemical shift of the corresponding DMF-coordinated species **4a** appearing at 51.9 ppm. Upon recording a series of ^{31}P NMR spectra of a chloroform solution of **15** containing increasing amounts of DMF, the pair of signals appearing at 46.7 and 47.2 ppm attributable to **15a** and **15b**, respectively, are progressively replaced by the signal at 49.8 attributable to **17**.

Figure 4. In situ $^{31}P\{^1H\}$ NMR study of the reaction between **18** and $Bu_3SnC{\equiv}CPh$ in $DMF{-}DMF{-}d_7$.

Scheme 3
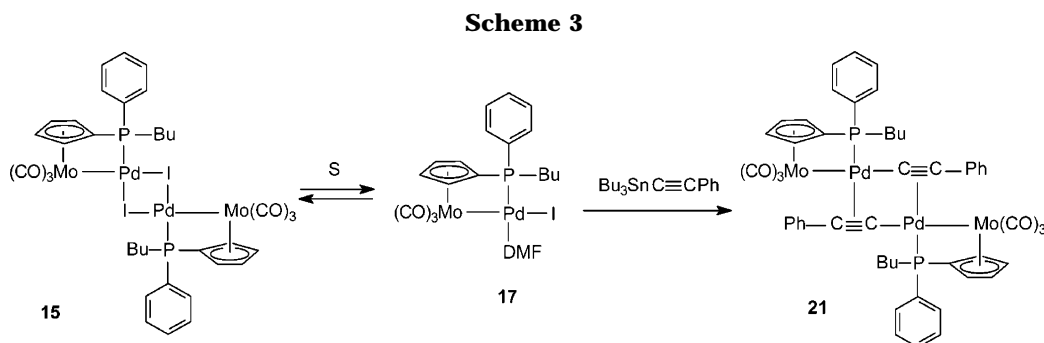
reactive species along the Pd-promoted coupling of aryl halides and vinylstannanes.[17]

The diastereomeric mixture **15** was reacted with PPh₃, yielding quantitatively a racemic mixture of the PPh₃ adduct **18**, which after workup was isolated in 83% yield (Scheme 2). The $^{31}P\{^1H\}$ NMR spectrum of **18** shows the typical four-line pattern and coupling constant expected for two *trans* phosphorus ligands (δ 37.6 and 18.8 ppm, $J = 434$ Hz). The ^1H NMR spectrum contains four different signals for the α, α', β, β' cyclopentadienyl protons, due to the presence of an adjacent chiral phosphorus atom. This magnetic anisotropy is also responsible for the diastereotopicity of the first two methylene groups of the butyl substituent.

Reactivity of 15 and 18 toward Organostannanes. In the attempt of getting additional mechanistic information on the catalytic cycle illustrated in Figure 2, $Bu_3Sn{-}C{\equiv}C{-}Ph$ was reacted with **18**, which may be described as the triphenylphosphine-stabilized product of the oxidative insertion of Pd^0 into the Mo$-$I moiety.

A preliminary experiment was performed in a 5 mm NMR tube and was followed by $^{31}P\{^1H\}$ NMR spectroscopy (Figure 4). In trace *a* of Figure 4 is reported the spectrum of **18** in DMF.[18] The spectrum reported in trace *b* has been recorded 10 min after the addition of 10 equiv of $Bu_3Sn{-}C{\equiv}C{-}Ph$. In addition to the signals of **18**, flanked by the characteristic four-line pattern due to the transmetalation product **20**,[19] two narrow doublets at 29.1 and 28.1 ppm ($J = 14$ Hz) appeared in the spectrum (**19**). The presence of these two doublets

persisted as long as the transformation of **18** into **20** was complete (trace *c*). A doublet of doublets was also observed during the reaction of $Bu_3Sn{-}C{\equiv}C{-}Ph$ with **2a,b** to give **7a,b** (Figure 2). It is therefore reasonable to conclude that the transient species **19** is just the Pd-π-alkyne adduct that ultimately converts to **20** with elimination of Bu_3SnI. All our attempts to isolate the transmetalation product **20** were unsuccessful due to its extreme sensitivity.[20]

The ability of the model metal iodide **14** to mimic the reactivity of the parent compound **1** (Figure 2) was further demonstrated by the direct reaction of **17**, generated by dissolving **15** in DMF, with $Bu_3Sn{-}C{\equiv}C{-}Ph$. Following this transformation by $^{31}P\{^1H\}$ spectroscopy showed that the singlet at 49.8 ppm due to **17** and the two signals at 47.7 and 47.4 ppm due to the tetrametallic species **15** disappeared within 40 min. Formed in their place was a pair of signals with very close chemical shifts, 24.85 and 24.90 ppm, attributable to the phosphine-free transmetalation species **21** (Scheme 3).

(17) Amatore, C.; Bahsoun, A. A.; Jutand, A.; Meyer, G.; Ndedi Ntepe, A.; Ricard, L. *J. Am. Chem. Soc.* **2003**, *125*, 4212.

(18) The reaction was carried out in DMF with addition of DMF-d_7 for lock purposes.

(19) Formation of **20** is accounted for by a doublet of doublets at 39.6 and 26.6 ppm, $J = 436$ Hz. This pattern is typical of a *trans* square-planar geometry around palladium.[4]

(20) The difficult to isolate transmetalation intermediates for this class of cyclopentadienylphosphino complexes were already experienced in a previous work.[4a]

Scheme 4
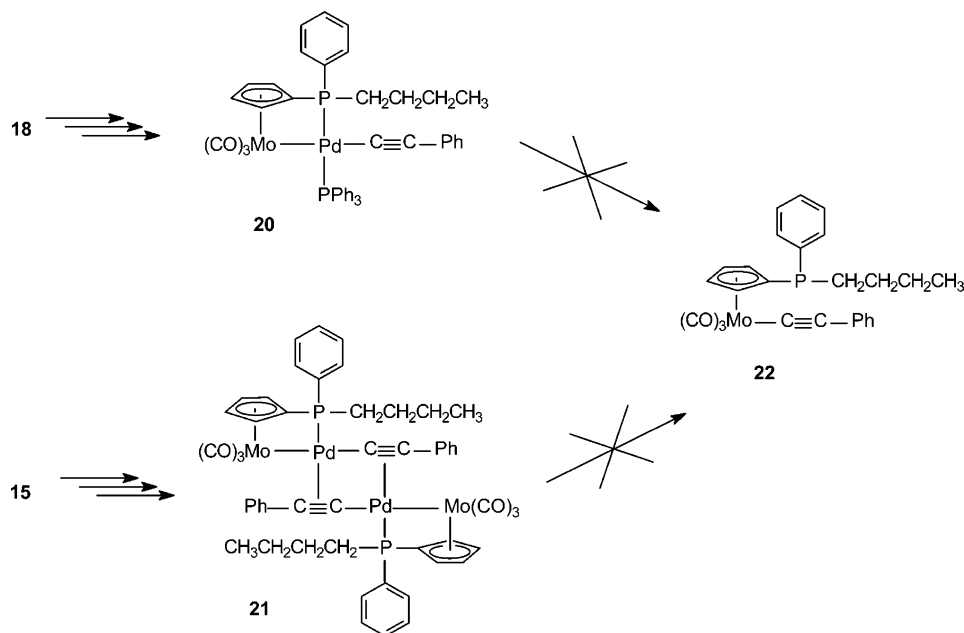
While the structure and the spectroscopic and chemical properties of **17** closely resemble those of the related compound **4a**, the slower rate observed for the transformation of **17** into **21**, as compared to the transformation of **4a** into **6a**, confirms that the nucleophilicity of the butyl-substituted phosphine controls the reactivity with tributyltinacetylides. In particular, the enhanced electron density at the P atom, besides slowing down the transmetalation reaction, also retards the overall catalytic rate, making more difficult the final reductive elimination step to give Mo$-$C$\equiv$CR. Indeed, under the conditions that allow the conversion of **7a** to **10a** via reductive elimination (Figure 2),[21] neither **20** nor **21** was converted to **22** (Scheme 4).[22,23]

Conclusions

With this work we have added new details in the complicated mosaic composing the mechanism of palladium-catalyzed bond-forming processes (Figure 2). By varying the steric requirements and the donor ability of the chelating cyclopentadienylphosphino moiety, it

has been possible to isolate and fully characterize an important intermediate (**15**), which is the precursor of either the highly reactive solvent-coordinated species **17** or the PPh$_3$-coordinated species **18**, which are both involved in key steps of the catalytic cycle. The central relevance of dimeric halobridged palladium species and of their highly reactive solvent-coordinated open forms (such as **5**, **15** and **4**, **17**) has been recently confirmed by Amatore[17] in Pd-catalyzed carbon$-$carbon bond-forming processes. In particular, substitution of a phenyl with a butyl group enhances the donor ability of the phosphine. This is reflected in an increased electron density on palladium and, as a consequence, in a lower reactivity toward nucleophiles (e.g., tin acetylides). In fact, formation of **20** and **21** by reaction of **18** and **17** with Bu$_3$Sn$-$C$\equiv$C$-$Ph is much slower than the corresponding reaction to form **7** and **6**.[4d] In addition, because of the enhanced donicity of phosphorus in **20** and **21**, palladium is more tightly retained, making reductive elimination difficult. Moreover, the absence of phenyl substituents on the cyclopentadienyl ring has an adverse effect on the stability of the transmetalation products **20** and **21**, which become nonisolable.

These results further support the mechanistic analogies between the palladium-promoted metal$-$carbon (M$-$C) bond formation process and the more conventional palladium-promoted carbon$-$carbon (C$-$C) coupling reaction, and in this respect, the overall picture outlined in Figure 2 offers a unique unifying view of these processes.

(21) Experimental conditions: **7**+Bu$_3$SnC$\equiv$CPh (10 equiv), 24 h, 60 °C in DMF.[4c]

(22) By following this transformation by ^{31}P NMR spectroscopy the disappearance of signals of starting material is accompanied by the formation of a species displaying a group of four doublets of doublets signals, which, upon prolonged warming, remain the only species in solution.

(23) To overcome reluctance of palladium to be extruded from **21**, the reductive elimination process was also carried out by treating **21** (formed according to the procedure outlined in Scheme 4) in the presence of bis-1,2-diphenylphosphinoethane (dppe). However, instead of acting as scavenging agent for Pd, thus favoring formation of **22** (Scheme 5), dppe added to **21** caused the formation of **23**, whose structure was assigned on the basis of spectroscopic data.
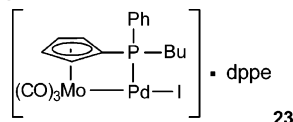
^{31}P{^{1}H} NMR (DMF/DMF-d_7, 121 MHz): AMX pattern, δ_A 56.3 (dd, J_{AM} = 47 Hz, J_{AX} = 368 Hz), δ_M 47.1 (dd, J_{AM} = 47 Hz, J_{MX} = 15 Hz), δ_X 30.3 (dd, J_{AX} = 368 Hz, J_{MX} = 15 Hz). MS (15 V, ESP$^+$): 915 (M $-$ I)$^+$, 830 (M $-$ I $-$ 3CO)$^+$.

Experimental Section

General Procedures. Elemental analyses were performed by the Servizio Microanalisi of the Dipartimento di Chimica, Università di Roma "La Sapienza". FT-IR spectra were recorded on a Nicolet 510 instrument in the solvent subtraction mode, using a 0.1 mm CaF$_2$ cell. [1]H, ^{13}C{^{1}H}, and ^{31}P{^{1}H} NMR spectra were recorded on a Bruker AC300P spectrometer at 300, 75, and 121 MHz, respectively. Chemical shifts (ppm) are reported in δ values relative to Me$_4$Si; for ^{1}H NMR, CHCl$_3$ (δ 7.24) or DMF (δ 2.90), and for ^{13}C NMR, CDCl$_3$ (δ 77.0) or

DMF-d_7 (δ 161.7) were used as internal standards. The ^{31}P-{^{1}H} NMR chemical shifts are relative to 85% H_3PO_4. Mass spectra were obtained on a Fisons Instruments VG-Platform Benchtop LC-MS (positive ion electrospray, ESP$^+$) spectrometer. Solvents, including those used for chromatography, were thoroughly degassed before use. Chromatographic separations were performed using 70–230 mesh silica gel (Merck). All manipulations were carried out under an atmosphere of argon with Schlenk type equipment on a dual-manifold argon/vacuum system. Liquids were transferred by syringe or cannula. THF was distilled from sodium–potassium alloy; DMF was distilled from CaH_2 under reduced pressure. (CH_3-$CN)_3Mo(CO)_3$ was prepared according to published procedures.[24] (C_5H_5)Tl, Cl_2PPh, BuLi, ICH_2CH_2I, Pd_2(dba)$_3$, Bu_3Sn–C≡C–Ph, and PPh$_3$ (Aldrich) were used as received.

Legend for ^{13}C NMR assignments:
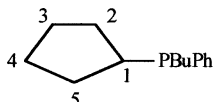
[Pd(μ-I){Mo(CO)$_3$(η^5-C$_5$H$_4$(PBuPh))}]$_2$ (15). A 250 mL Schlenk flask was loaded with 0.81 g (2.9 mmol) of thallium cyclopentadienide. After three cycles of vacuum/argon, 80 mL of THF was added to the flask and then 0.4 mL (2.9 mmol) of dichlorophenylphosphine, causing the formation of a white precipitate of thallium chloride. The reaction mixture was stirred for 30 min at room temperature. The resulting pale yellow solution was filtered, and the residue on the filter was washed four times with 20 mL portions of THF. After cooling at 0 °C, BuLi (1.6 M solution in hexanes) (4.0 mL, 6.4 mmol) was added to the filtrate, and after 30 min, 2.53 g (3.2 mmol) of ($CH_3CN)_3Mo(CO)_3$ was added as a solid. A green-brown solution was obtained. After stirring overnight at room temperature, a 2 h reflux, and cooling at room temperature, 0.90 g (3.2 mmol) of solid 1,2-diiodoethane was added. The resulting deep red solution was stirred for 1 h. Following addition of 1.56 g (1.5 mmol) of Pd_2(dba)$_3$ and after 1 h stirring, Celite was added to the solution and the solvent removed under vacuum. The coated residue was chromatographed on a silica column (45 cm × 3 cm). Elution with *n*-hexane–dichloromethane (4:6) produced a red band, which was eluted and collected to give, after removal of the solvent, 0.39 g (21%) of **15**, as a red-bordeaux crystalline solid.

Recrystallization from CH_2Cl_2–pentane (liquid diffusion) at room temperature gave bright red needle crystals. ^{1}H NMR (CDCl$_3$): δ 8.23–8.13 (m, 8H, *o*-Ph), 7.54–7.48 (m, 4H, *p*-Ph), 7.44–7.38 (m, 8H, *m*-Ph), 5.48 (m, 4H), 5.42 (m, 2H), 5.39 (m, 2H), 4.97 (m, 4H), 4.16 (m, 2H), 4.13 (m, 2H) (Cp), 2.79–2.64, 2.40–2.24 (m, 8H, C*H₂*CH₂CH₂CH₃), 2.13–1.97, 1.68–1.55 (m, 8H, CH₂C*H₂*CH₂CH₃), 1.51–1.38 (m, 8H, CH₂CH₂C*H₂*CH₃), 0.92 (t, 6H, $J = 6.7$ Hz, CH₂CH₂CH₂C*H₃*), 0.91 (t, 6H, $J = 6.7$ Hz, CH₂CH₂CH₂C*H₃*). ^{31}P{^{1}H} NMR (CDCl$_3$): δ 47.2 (s), 46.7 (s). ^{13}C{^{1}H} NMR (DMF-d_7): δ 238.6, 224.0, 223.1 (CO), 135.5 (d, $J_{C-P} = 12.6$ Hz), 131.8 (d, $J_{C-P} = 3.6$ Hz), 128.5–127.8, 127.3, 93.2–92.9 (Ph + Cp), 60.2 (d, $J_{C-P} = 44.9$ Hz, C$_1$), 30.7 (d, $J_{C-P} = 37.7$ Hz, *C*H₂CH₂CH₂CH₃), 28.1 (d, $J_{C-P} = 3.6$ Hz, CH₂CH₂*C*H₂CH₃), 23.6 (d, $J_{C-P} = 18.0$ Hz, CH₂*C*H₂CH₂CH₃), 12.7 (s, CH₂CH₂CH₂*C*H₃). FT-IR (CH₂Cl₂, cm^{-1}): 1975, 1895 (ν_{CO}). MS (15V, ESP$^+$): *1158* (M − I)$^+$, *1130* (M − I − CO)$^+$.

[Pd(I)(PPh$_3$){Mo(CO)$_3$(η^5-C$_5$H$_4$(PBuPh))}] (18). A 100 mL Schlenk flask was loaded with 86 mg (0.0669 mmol) of complex **15** and 35.1 mg (0.134 mmol) of PPh$_3$. Following three cycles of vacuum/argon, 10 mL of THF was added to the flask

and the mixture was stirred at room temperature. After 30 min Celite was added to the solution and the solvent was removed under vacuum. The coated residue was chromatographed on a silica column (35 cm × 2.5 cm). Elution with *n*-hexane–dichloromethane (4:6) produced a red band, which was collected to give, after removal of the solvent under vacuum, 102 mg (83%) of **18**, as red solid. ^{1}H NMR (DMF-d_7): δ 8.23–8.17 (m), 7.90–7.40 (Ph), 5.81 (s, 1H), 5.70 (s, 1H), 5.45 (s, 1H), 4.20 (s, 1H), (Cp), 3.38–3.25, 2.79–2.64 (m, 2H, C*H₂*-CH₂CH₂CH₃), 2.18–2.04, 1.76–1.63 (m, 2H, CH₂C*H₂*CH₂CH₃), 1.50 (sex, 2H, $J = 7.4$ Hz, CH₂CH₂C*H₂*CH₃), 0.97 (t, 3H, $J = 7.4$ Hz, CH₂CH₂CH₂C*H₃*). ^{31}P{^{1}H} NMR (DMF-d_7): δ 37.6 (d, $J_{P-P} = 434$ Hz), 18.8 (d, $J_{P-P} = 434$ Hz). ^{13}C{^{1}H} NMR (DMF-d_7): δ 236.6, 225.5, 224.7 (CO), 135.4–127.6, 93.6–92.9 (Ph + Cp), 59.4 (d, $J_{C-P} = 37.7$ Hz, C$_1$), 33.9 (d, $J_{C-P} = 32.3$ Hz, *C*H₂CH₂CH₂CH₃), 28.3 (s, CH₂CH₂*C*H₂CH₃), 24.0 (d, $J_{C-P} = 16.2$ Hz, CH₂*C*H₂CH₂CH₃), 12.9 (s, CH₂CH₂CH₂*C*H₃). FT-IR (CH₂Cl₂, cm^{-1}): 1963, 1889 (sh), 1866 (ν_{CO}). Anal. Calcd for C₃₆H₃₃IMoO₃P₂Pd: C, 47.79; H, 3.68. Found: C, 47.81; H, 3.67.

X-ray Diffraction Study. A parallelepiped crystal with dimensions 0.47 × 0.12 × 0.10 mm was used for the data collection. Experimental data were recorded at room temperature (20 °C) on an Philips-Febo PW1100. A set of 25 carefully centered reflections in the range $11.5° \leq \theta \geq 19.5°$ was used for determining the lattice constants. As a general procedure, the intensity of three standard reflections was measured periodically every 200 reflections for orientation and intensity control. This procedure did not reveal decay of intensities. The data were corrected for Lorentz and polarization effects. Atomic scattering factors were taken from A. J. C. Wilson[25a] with anomalous dispersion corrections taken from ref 25b. An empirical absorption correction was applied via Ψ scan with correction factors in the range 2.951–1.009. The computational work was carried out by using the program SHELX97.[26] Final atomic coordinates of all atoms and structure factors are available on request from the authors and are provided as Supporting Information. The structure was solved by direct methods using the SIR97 program.[27] The refinement was done by full-matrix least-squares calculations, initially with isotropic thermal parameters, then with anisotropic thermal parameters for all the atoms. Hydrogen were introduced at calculated positions. The phenyl ring was treated as a rigid body with D_{6h} symmetry, and the hydrogen atoms were allowed to ride on the attached carbon atoms.

Supporting Information Available: Figures showing *rac dl* (**15a**) and *meso* (**15b**) diastereomers, ^{31}P{^{1}H} NMR of **15**, and ^{1}H NMR of **15** and **18**. Full tables of crystal data, atomic coordinates, thermal parameters, and bond lengths and angles for **15b**. This material is available free of charge via the Internet at http://pubs.acs.org.

OM0400595

(24) Tate, D. P.; Knipple, W. R.; Augl, J. M. *Inorg. Chem.* **1962**, *1*, 433.

(25) Wilson, A. J. C. *International Tables for X-Ray Crystallography*; Kluwer Academic: Dordrecht, 1992; Vol. C, p 500. (b) Wilson, A. J. C. *International Tables for X-Ray Crystallography*; Kluwer Academic: Dordrecht, 1992; Vol. C, p 219.

(26) Sheldrick, G. M. *SHELX97. Program for Crystal Structure Determination*; University of Göttingen: Germany, 1997.

(27) Altomare, A.; Burla, M. C.; Camalli, M.; Cascarano, G.; Giacovazzo, C.; Guagliardi, A.; Polidori, G.; Spagna, R. *J. Appl. Crystallogr.* **1999**, *32*, 115.